Article

Discovery Medicine 2025; 37(193): 315–325
https://doi.org/10.24976/Discov.Med.202537193.25

ELF1's Role in Colorectal Cancer: Up-Regulating DCLK1 Expression to Propel Malignant Progression and Stemness Features

Dongai Zhou[1,2,3], Xiaocai Tian[1,2,3], Hong Yang[1,2,3], Shengying Xiao[1,2,3], Yichen Lu[1,2,3], Furen Zeng[1,2,3,*]

[1]Department of Oncology, Hunan Provincial People's Hospital, 410002 Changsha, Hunan, China
[2]Key Laboratory of Small Molecule Targeted Drug Research and Creation in Hunan Province, 410002 Changsha, Hunan, China
[3]Hunan Provincial Clinical Medical Research Center for Hepatobiliary Pancreatic Tumors, 410002 Changsha, Hunan, China
*Correspondence: zengfrhn@163.com (Furen Zeng)
Published: 20 February 2025

Background: Exploring the pathological mechanism of colorectal cancer (CRC) onset and advancement is critical to clinical diagnosis and treatment. In this context, our study brings a novel perspective by investigating the role and regulatory mechanism of E74 Like ETS Transcription Factor 1 (*ELF1*) in CRC, a topic that has not been extensively explored.
Methods: Quantitative reverse transcription polymerase chain reaction (RT-qPCR) and western blotting (WB) assays were used to detect the expression of ELF1 in CRC cells. Sh-ELF1, ELF1 overexpresses lentivirus (Oe-ELF1), and Oe-Doublecortin Like Kinase 1 (DCLK1) were constructed and transfected into CRC cells. Transfection efficiency and the expression of stemness, as well as epithelial-mesenchymal transition (EMT)-related proteins were detected using RT-qPCR and WB assays. Cell proliferation and sphere-forming ability were detected using Cell Counting Kit-8 (CCK-8) assay, 5-Ethynyl-2′-deoxyuridine (EdU) staining, and sphere formation assay. Cell migration and invasion were detected using wound healing and transwell assay. The tube-forming ability of human umbilical vein endothelial cells (HUVEC) cells was detected using tubular formation experiments. To investigate the regulatory mechanism of ELF1, the crosstalk between ELF1 and downstream DCLK1 was predicated and verified using the JASPAR database, luciferase reporter gene, and Chromatin Immunoprecipitation (ChIP) assay.
Results: Results of the present study demonstrated that ELF1 expression was upregulated in CRC cells ($p < 0.001$). ELF1 silence significantly inhibited CRC cell proliferation, stemness, invasion, migration, and angiogenesis ($p < 0.001$). ELF1 silence also suppressed the expressions of Nanog Homeobox (Nanog), SRY-Box Transcription Factor 2 (Sox2), Octamer-Binding Transcription Factor 4 (OCT4), N-cadherin, and Vimentin while increasing the expression of E-cadherin ($p < 0.001$). Besides, ELF1 could positively regulate DCLK1 expression. However, the results of subsequent experiments revealed that DCLK1 overexpression partially offset the inhibitory effects of ELF1 knockdown on CRC cell proliferation, stemness, invasion, migration, and angiogenesis ($p < 0.01$).
Conclusion: In summary, our study provides compelling evidence that ELF1 up-regulates DCLK1 expression, thereby promoting the malignant progression and stemness of colorectal cancer. These findings significantly contribute to our understanding of the regulatory mechanisms in CRC and may have implications for future therapeutic strategies.

Keywords: ELF1; DCLK1; colorectal cancer; malignant progression; stemness

Introduction

Colorectal cancer (CRC) is a prevalent aggressive digestive tumor [1,2]. Until now, the infiltration and metastasis of malignant tumors have been widely investigated at the cellular and molecular levels, and a variety of abnormal expression genes related to malignant tumor metastasis have been found [3]. Therefore, further exploring the mechanism of CRC onset and advancement at the molecular level and discovering more specific molecular markers and therapeutic targets are of great significance.

Previous research has identified E74 Like ETS Transcription Factor 1 (*ELF1*) as a predictor of CRC outcome [4]. In addition, Transmembrane 9 Superfamily Member 2 (*TM9SF2*), which *ELF1* transcriptionally regulates, is likely to function as an oncogene by significantly affecting CRC tumorigenesis [5]. ELF1 can be widely found in various eukaryotes. It is found that ELF1 proteins are similar in structure and evolutionarily conserved in eukaryotes, constituting one transcription factor extension family [6]. However, the expression of ELF1 in CRC and its specific regulatory mechanism has not been reported thus far. *ELF1* has been considered to play an important role in

regulating carcinogenesis and tumor advancement. *ELF1* transcription factor promotes glioma progression through the Activating Transcription Factor 5 (*ATF5*) promoter [7]. *ELF1* facilitates the transcription of Forkhead Box D3 Antisense RNA 1 (*FOXD3-AS1*) to promote the metastasis of osteosarcoma cells [8]. Therefore, this study aimed to investigate ELF1 expression and its reaction mechanism on tumor growth in CRC.

Materials and Methods

Databases

ELF1 expression in CRC patients was predicted by the UALCAN web tool (https://ualcan.path.uab.edu/analysis.html) [9]. JASPAR database (https://jaspar.genereg.net/) predicted the binding sites of transcription factors *ELF1* and Doublecortin Like Kinase 1 (*DCLK1*) promoters [10].

Cell Lines and Culture

Human intestinal epithelial cells (HIEC-6, YS3102C) were obtained from Shanghai Yaji Biotechnology Co., Ltd. (Shanghai, China). Human umbilical vein endothelial cells (HUVECs, BNCC342438) and CRC cells, including Caco2 (BNCC350769), LoVo (BNCC338601), SW480 (BNCC100604) and HCT116 (BNCC287750) cells were obtained from BeNa Culture Collection (Suzhou, China). All cells were grown in Dulbecco's modified eagle medium (DMEM) (11965-092, Gibco, Thermo Fisher Scientific, Waltham, MA, USA) containing 10% fetal bovine serum (FBS, Gibco, Thermo Fisher Scientific, Germany) and 1% penicillin-streptomycin (P1400, Solarbio, Beijing, China). The cells were maintained at 37 °C in a humidified atmosphere of 5% CO_2 and were used during their logarithmic growth phase. All cells have been identified by short tandem repeat (STR) and tested for mycoplasma, and all experiments were performed under sterile conditions.

Quantitative Reverse Transcription Polymerase Chain Reaction (RT-qPCR)

The total RNA was extracted using Trizol reagent (15596026, Invitrogen, Carlsbad, CA, USA), and mRNA level was examined with SYBR Green qPCR Master Mix (HY-K0501, MCE, USA) according to the manufacturer's instructions. Relative gene expression was calculated using the $2^{-\Delta\Delta Ct}$ [11] method and normalized to glyceraldehyde-3-phosphate dehydrogenase (GAPDH). The primer sequences for this study were obtained from PrimerBank and are as follows: *ELF1*, F-5′-TGTGGAAGAGCCCAATGACAT-3′, R-5′-AGCTTCAACTGTAAGGGTGATG-3′; *DCLK1*, F-5′-ACTTCGACGAGCGGGATAAG-3′, R-5′-GGGCCTCAAAAGATCGGAACC-3′; *GAPDH*, F-5′-CTGGGCTACACTGAGCACC-3′, R-5′-AAGTGGTCGTTGAGGGCAATG-3′.

Western Blotting

Total proteins were extracted using radioimmunoprecipitation assay (RIPA) buffer (PC102, Epizyme Biomedical Technology, Shanghai, China) and separated by sodium dodecyl sulfate-polyacrylamide gel electrophoresis (SDS-PAGE, G2037-50T, Servicebio Biotechnology, Wuhan, China). An equal amount of proteins (40 µg proteins per lane) were transferred onto polyvinylidene fluoride (PVDF) membranes. After the inhibition with 5% bovine serum albumin (BSA, BS114, biosharp, Hefei, China) sealing solution for 2 h at room temperature, the membranes were incubated with primary antibodies overnight at 4 °C. Primary antibodies included anti-ELF1 (1:1000, ab64937, Abcam, Cambridge, UK), anti-DCLK1 (1:1000, ab31704, Abcam), anti-Nanog Homeobox (anti-Nanog), (1:1000, ab109250, Abcam), anti-SRY-Box Transcription Factor 2 (anti-Sox2) (1:1000, ab92494, Abcam), anti-Octamer-Binding Transcription Factor 4 (anti-OCT4) (1:1000, ab181557, Abcam), anti-E-cadherin (1:1000, ab231303, Abcam), anti-N-cadherin (1:1000, ab76011, Abcam), anti-Vimentin (1:1000, ab92547, Abcam), beta-actin (1:1000, ab8227, Abcam) and glyceraldehyde-3-phosphate dehydrogenase (GAPDH, 1:1000, ab9485, Abcam). On the next day, the membranes were incubated with secondary antibodies goat anti-rabbit immunoglobulin G (goat anti-rabbit IgG, 1:5000, ab150077, Abcam) and goat anti-mouse IgG (1:5000, ab205719, Abcam) for 2 h at room temperature. Enhanced chemiluminescence (ECL) reagent (P1000-25, Applygen, Beijing, China) was adopted for immunoreactive signal analysis, and Image Lab software (Version 1.6, Bio-Rad, Hercules, CA, USA) was applied for blot quantification. The relative protein expression was calculated according to the gray value of the target protein/gray value of the internal reference protein.

Cell Transfection

HCT116 cells were cultured in 24-well plates at a density of 2×10^5 and infected with lentivirus expressing ELF1 (sh-ELF1#1, 5′-CCTGCCGTAATTGTGGAACAT-3′; sh-ELF1#2, 5′-ATGTTCCTGGTGCTGATATTC-3′), ELF1 overexpresses lentivirus (Oe-ELF1) and Oe-DCLK1, and the corresponding negative controls sh-NC (5′-TCGTTGGCACTTCGGGTC-3′) and Oe-NC (Shanghai Genechem Co., Ltd.) using Hieff Trans® transfection reagent (40802ES08, Yeasen, Shanghai, China) according to the manufacturer's instructions. After 48 h, the transfected cells were harvested for the following experiments. RT-qPCR or western blotting assessed the transfection efficacy.

Counting Cell Kit-8 (CCK-8)

Following the injection onto 96-well plates (5×10^3 per well), cells were incubated for indicated times (24, 48, 72 h) with 10 µL of CCK-8 (CA1210, Solarbio, Beijing,

China). The absorbance at 450 nm was detected using a spectrophotometer (DS-7, DeNovix, Wilmington, Germany).

5-Ethynyl-2′-Deoxyuridine (EdU) Staining

Following the injection into 96-well plates (1×10^5 per well), cells were incubated with 20 µM EdU (E2051; Applygen, Beijing, China) for 2 h. After glycine neutralization, cells were immobilized with 4% paraformaldehyde (BL539A, Biosharp, Hefei, China) for 30 min and permeated in 0.5% TritonX-100 (E2051; Applygen, Beijing, China) for 10 min. Then, cells were exposed to a click reaction solution (E2051; Applygen, Beijing, China) for 30 min, and Hoechst 33342 (E2051; Applygen, Beijing, China) was applied to visualize cell nuclei. The positive cells were observed by a fluorescent microscope (DM IL LED, Leica, Wetzlar, Germany).

Tumor Sphere Formation Assay

Following the resuspension in a conditioned medium supplemented with 5 µg/mL insulin, 20 ng/mL EGF, 2% B27, and 20 ng/mL basic fibroblast growth factor. The size of spheres was measured under an optical microscope at 10× magnification (BMF-100, Olympus, Tokyo, Japan) and quantified using Image J version 1.6 software (National Institutes of Health, Bethesda, MD, USA).

Tubule Formation Assay

The conditioned medium (CM) was prepared by the supernatants of HCT116 cells with indicated treatment. Next, HUVECs in 100 µL CM were seeded in a Matrigel-coated 96-well plate (4×10^4 cells/ well). After 24 h, the formed tubes were monitored using a light microscope (BX3M, Olympus).

Luciferase Reporter Assay

HCT116 cells were infected with the dual luciferase reporter vectors containing mutated or wild DCLK1 3′-UTR region (DCLK1-WT or DCLK1-MUT) and Oe- ELF1 or Oe-NC. A Dual Glo Luciferase Reporter Gene Assay Kit (11405ES60, Yeasen, Shanghai, China) was utilized to confirm the luciferase activities after transfection for 48 h. The luciferase luminescence signal was detected by a luminescence detector (GloMax® 20/20 Luminometer System, Promega, Madison, WI, USA).

Chromatin Immunoprecipitation (ChIP) Analysis

The enrichment of the DCLK1 promoter in the ELF1 antibody was detected using Chromatin Immunoprecipitation Kit (P2179S, Beyotime, Shanghai, China) according to the manufacturer's instructions. Briefly, DNA fragments of 200–500 bp were produced after the sonication of HCT116 cells. Then, following the incubation with 20 µL of protein A/G magnetic beads (P2179S, Beyotime, Shanghai, China), the precleared chromatin was exposed to ELF1 (A301-443A, Invitrogen) or IgG (ab172730, Abcam) antibodies (4 µg) at 4 °C overnight with rotation. The magnetic beads-antibody-protein-DNA complexes were thoroughly washed with the lysate containing the inhibitor, and the protein-DNA complexes were purified and eluted. PCR was used to examine the enrichment efficiency of DCLK1 in protein-DNA complexes.

Wound Healing

HCT116 cells were injected into 96-well plates (1×10^5 per well), and then an incision-like gap was created using a 200 µL pipette. Three randomly selected gaps were selected and photographed via a light microscope (BX3M, Olympus). After 24 h, Image J version 1.6 software (National Institutes of Health, Bethesda, MD, USA) was used to quantify the migration rate. Cell migration rate was calculated as cell migration rate = (initial scratch area – scratch area after 24 hours)/initial scratch area × 100%.

Transwell

Firstly, Matrigel (500 ng/mL, Corning Costar, Corning, NY, USA) was added to the upper chamber of the Transwell and incubated at °37C for 2 hours to allow it to solidify. Then, the superior 24-well transwell chamber (Corning Incorporated, Corning, NY, USA) was injected with 10,000 HCT116 cells resuspended in a serum-free medium, while the bottom chamber was supplemented with a medium containing 10% FBS. Following 48 h at °37C, the chambers were fixed with 4% paraformaldehyde at room temperature for 30 min and stained with 0.1% crystal violet at room temperature for 10 min. The invaded cells were observed under a microscope and analyzed using Image J version 1.6 software (National Institutes of Health, Bethesda, MD, USA).

Statistical Analysis

The collected data were processed with SPSS version 19.0 software (International Business Machines Corporation, Armonk, NY, USA) and presented as means and standard deviation (SD). One-way analysis of variance (ANOVA) with Tukey's test was used to compare the differences. $p < 0.05$ indicated statistical significance.

Results

ELF1 is Highly Expressed in CRC

UALCAN database predicted that ELF1 expression was upregulated in tissues of CRC patients (Fig. 1A, $p < 0.001$). RT-qPCR and western blotting examined ELF1 expression in CRC cells, and the data revealed that compared with the HIEC-6 cells, ELF1 expression in CRC cells was significantly increased (Fig. 1B, $p < 0.001$). HCT116 cells were selected for subsequent experiments because HCT116 cells had the highest expression of ELF1.

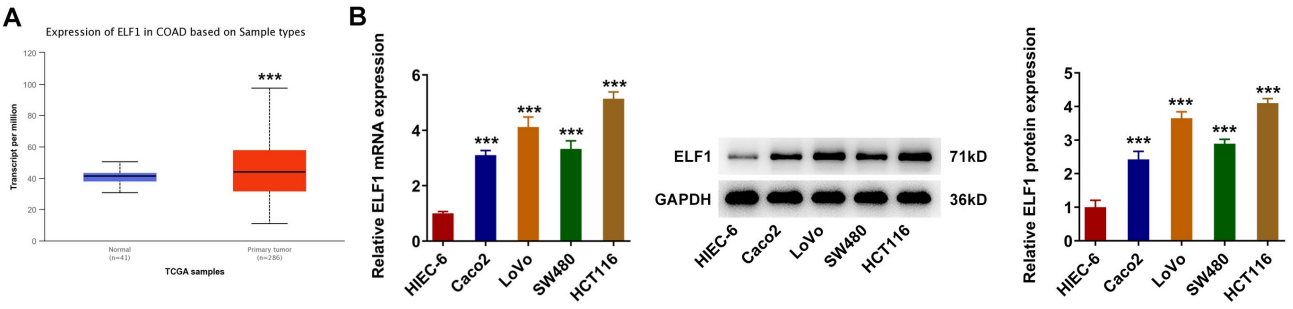

Fig. 1. ELF1 is highly expressed in colorectal cancer (CRC). (A) The UALCAN database showed that ELF1 was highly expressed in the tissues of CRC patients. (B) The expression of ELF1 in CRC cells was detected by quantitative reverse transcription polymerase chain reaction (RT-qPCR) and western blotting (n = 3). ***$p < 0.001$ vs HIEC-6. ELF1, E74 Like ETS Transcription Factor 1; GAPDH, glyceraldehyde-3-phosphate dehydrogenase.

Interference with ELF1 Inhibits CRC Proliferation and Stemness

Next, we constructed *ELF1* interference plasmid and divided HCT116 cells into a control group, sh-NC group, sh-ELF1#1 group, and sh-ELF1#2 group. RT-qPCR and western blotting results showed that ELF1 expression was lower in the sh-ELF1#2 group than in the sh-ELF1#1 group. Therefore, we chose sh-ELF1#2 (hereafter referred to as sh-ELF1) for subsequent experiments (Fig. 2A, $p < 0.001$). Cell viability was measured using CCK-8 assay, and it was found that *ELF1* interference significantly reduced cell viability (Fig. 2B, $p < 0.001$). Results of EdU staining showed that compared with the sh-NC group, cell proliferation in the sh-ELF1 group was significantly decreased (Fig. 2C, $p < 0.01$). Sphere formation assay detected the sphere-forming ability of HCT116 cells, and the data disclosed that the sphere-forming capacity of HCT116 cells was inhibited by *ELF1* knockdown (Fig. 2D). Cell stem-related proteins were detected using western blotting, and it was found that the expressions of Nanog, Sox2, and OCT4 were significantly decreased in the sh-ELF1 group compared with the sh-NC group (Fig. 2E, $p < 0.001$).

ELF1 Deletion Inhibits the Invasion, Migration, and Angiogenesis of CRC Cells

Migration and invasion ability were measured via wound healing and Matrigel invasion assay, and it was found that cell migration and invasion were significantly inhibited by *ELF1* silence (Fig. 3A,B, $p < 0.001$). Subsequent western blotting results of ETM-related proteins showed that E-cadherin expression increased compared to the sh-NC group. In contrast, N-cadherin and Vimentin expressions were decreased in the sh-ELF1 group (Fig. 3C, $p < 0.001$). Moreover, the tubule formation assay results showed that *ELF1* interference inhibited the tubule formation ability of HUVECs (Fig. 3D, $p < 0.001$).

ELF1 Promotes the Transcription of DCLK1

The binding sites in the DCLK1 promoter with ELF1 transcription factor were predicted by the JASPAR database (Fig. 4A). Results obtained from RT-qPCR and western blottingting revealed that DCLK1 expression was increased in HCT116 cells compared with the HIEC-6 cells (Fig. 4B, $p < 0.001$). Compared with the Oe-NC group, ELF1 expression was significantly increased in the Oe-ELF1 group (Fig. 4C, $p < 0.001$). Luciferase results revealed that the DCLK1 promoter activity was increased by *ELF1* overexpression (Fig. 4D, $p < 0.001$). ChIP assay showed that the DCLK1 promoter was enriched in the anti-in ELF1 group (Fig. 4E, $p < 0.001$). Finally, it was discovered that DCLK1 expression was increased when *ELF1* was overexpressed, while DCLK1 expression was significantly decreased when ELF1 was silenced in CT116 cells (Fig. 4F, $p < 0.01$).

ELF1 Up-Regulates DCLK1 Expression and Promotes Malignant Progression and Stemness of CRC

DCLK1 overexpression plasmid was constructed, and RT-qPCR and western blotting successfully testified to the transduction efficacy (Fig. 5A, $p < 0.001$). Subsequently, the cells were divided into Control, sh-ELF1, sh-ELF1 + Oe-NC, and sh-ELF1 + Oe-DCLK1 groups. Cell viability and proliferation were tested, and the inhibited cell proliferation due to ELF1 deletion was partially revived by DCLK1 overexpression (Fig. 5B,C, $p < 0.05$). Sphere formation assay substantiated that compared with the sh-ELF1 + Oe-NC group, the sphere-forming ability of HCT116 cells in the sh-ELF1 + Oe-DCLK1 group was significantly increased (Fig. 5D). Western blotting was applied for the measurement of stem-related proteins, and it was found that Nanog, Sox2, and OCT4 expressions in the sh-ELF1 + Oe-DCLK1 group were significantly increased compared with the sh-ELF1 + Oe-NC group (Fig. 5E, $p < 0.01$). Results of wound healing and transwell assay illustrated that *DCLK1* overexpression might counteract the inhibitory effects of ELF1 interference on CRC cell migration and invasion (Fig. 6A,B,

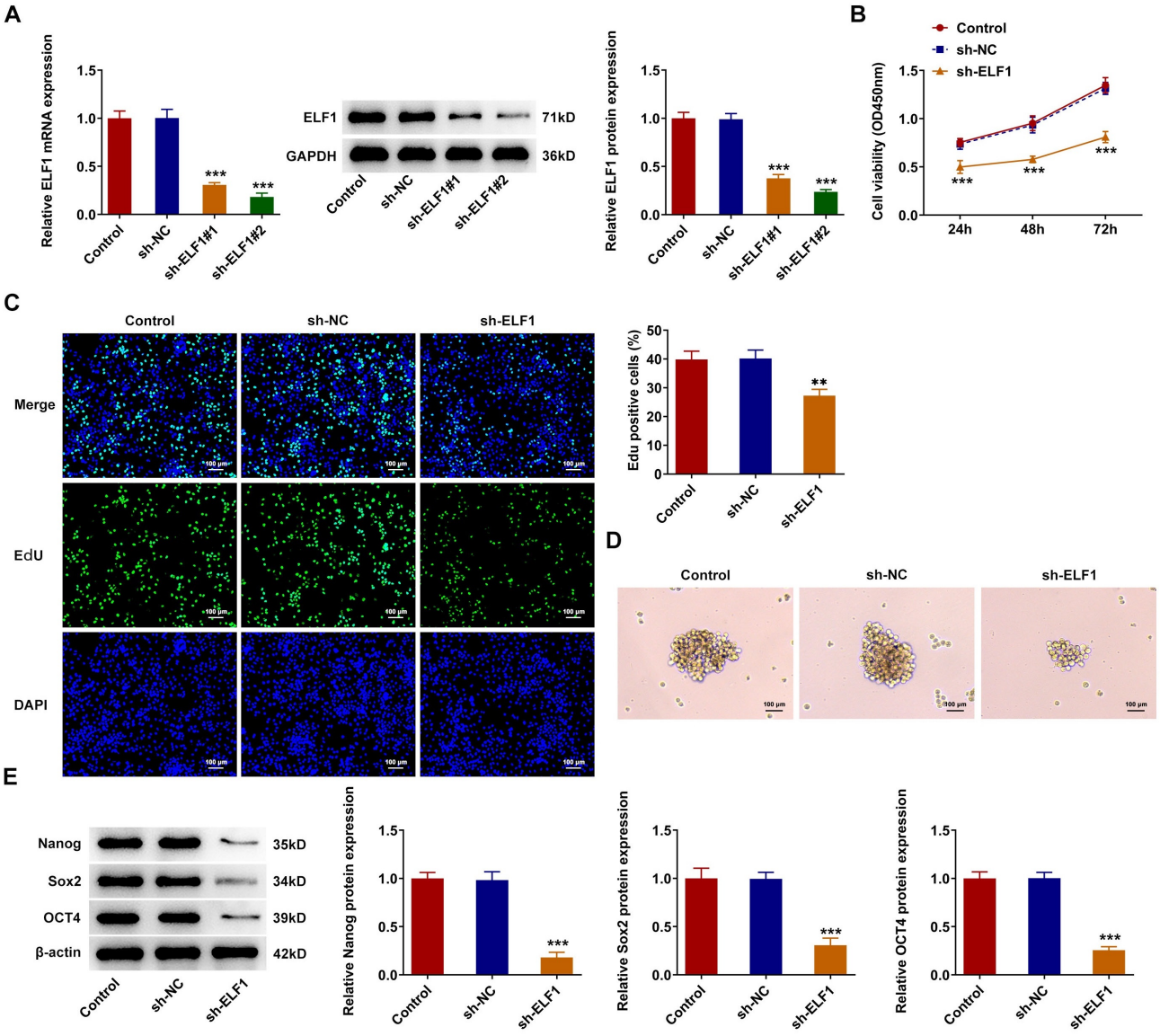

Fig. 2. Interference with ELF1 inhibits the proliferation and stemness of CRC cells (n = 3). (A) The transfection efficiency of ELF1 was detected by RT-qPCR and western blotting. (B) Cell viability was measured by Cell Counting Kit-8 (CCK-8) assay. (C) EdU staining detected cell proliferation (100 μm). (D) Sphere formation assay detected the sphere-forming ability of CRC cells (100 μm). (E) Western blotting analysis detected the expressions of cell stem-related proteins Nanog, Sox2, and OCT4. $^{**}p < 0.01$, $^{***}p < 0.001$ vs. sh-NC. EdU, 5-Ethynyl-2′-deoxyuridine; Sox2, SRY-Box Transcription Factor 2; Nanog, Nanog Homeobox; OCT4, Octamer-Binding Transcription Factor 4; DAPI, 4',6-diamidino-2-phenylindole.

$p < 0.001$). In addition, compared with the sh-ELF1 + Oe-NC group, E-cadherin expression was decreased in the sh-ELF1 + Oe-DCLK1 group, while N-cadherin and Vimentin expression was increased (Fig. 6C, $p < 0.01$). Compared with the sh-ELF1 + Oe-NC group, DCLK1 overexpression significantly increased the tubule-forming ability of HUVECs (Fig. 6D, $p < 0.001$).

Discussion

Due to the accumulation of mutations, cell proliferation is uncontrolled, which is the cause of malignant tumors. Tumor stem cells play important roles in mutated cell subsets. Stemness is often used to indicate tumor stem cell self-renewal and differentiation in malignant tumors [12]. The study has shown that the stemness of malignant tumors can affect tumor growth, angiogenesis, and other biological characteristics, thus promoting tumor invasion [13]. Therefore, it is an effective treatment strategy to inhibit malignant tumors' proliferation, invasion, migration, and stemness. In this paper, we explored the mechanisms by which *ELF1* regulated the malignant progression and the stemness of CRC, which might lay a theoretical foundation for CRC-targeted therapy in the clinic. The results showed that

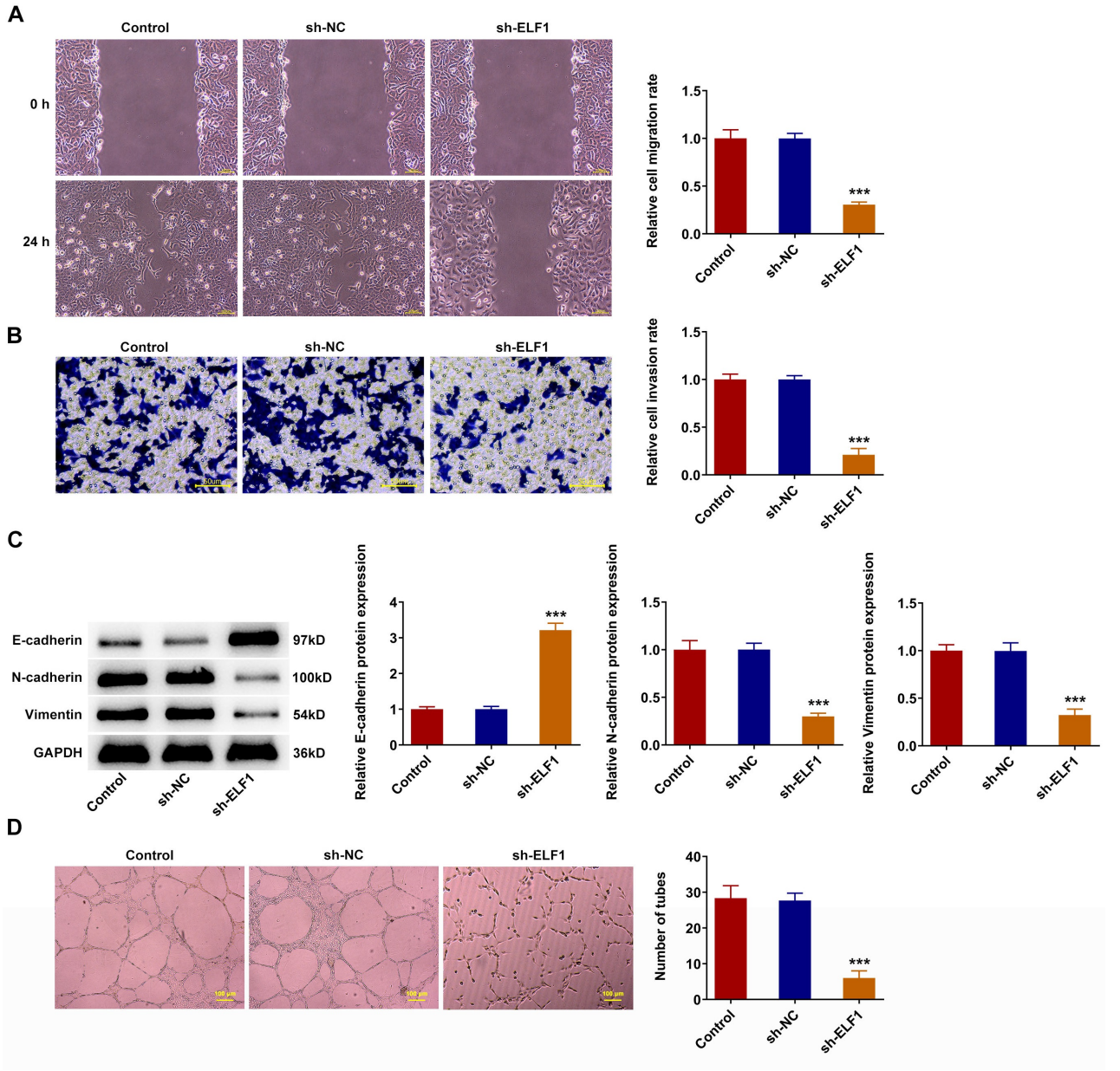

Fig. 3. Interference with ELF1 inhibits CRC cells' invasion, migration, and angiogenesis (n = 3). The migration and invasion ability of CRC cells were measured by wound healing (A, 100 μm) and transwell assay (B, 50 μm). (C) Western blotting detected the expressions of ETM-related proteins. (D) Tubule formation assay detected tubule forming ability of HUVECs (100 μm). ***$p < 0.001$ vs. sh-NC.

ELF1 up-regulates DCLK1 expression, thereby promoting the malignant progression and stemness of CRC.

According to UALCAN database prediction, ELF1 expression was predicted to be up-regulated in CRC patients, and this study found that ELF1 expression was significantly increased in CRC cells through cellular experiments. *ELF1* has been documented to play significant roles in cancer. LUCAT1 mediated by ELF1 promotes choroidal melanoma advancement via RBX1 [14]. *ELF1* is involved in the ceRNA network composed of SNHG17 and miR-384 to transcriptionally modulate CTNNB1 and serve as an activator of the Wnt/beta-catenin pathway to promote oral squamous cell carcinoma cell growth [15]. Nonetheless, there is little literature regarding the function and reaction mechanism of *ELF1* in CRC. This study revealed that after silencing *ELF1* expression, HCT116 cell viability was decreased, and cell proliferation and sphere-forming capacities were significantly inhibited, accompanied by reduced expressions of stem-related proteins Nanog, Sox2, and OCT4. In addition, interference with *ELF1* significantly inhibited the invasion, migration, and angiogenesis of HCT116 cells. Our experimental results are consistent

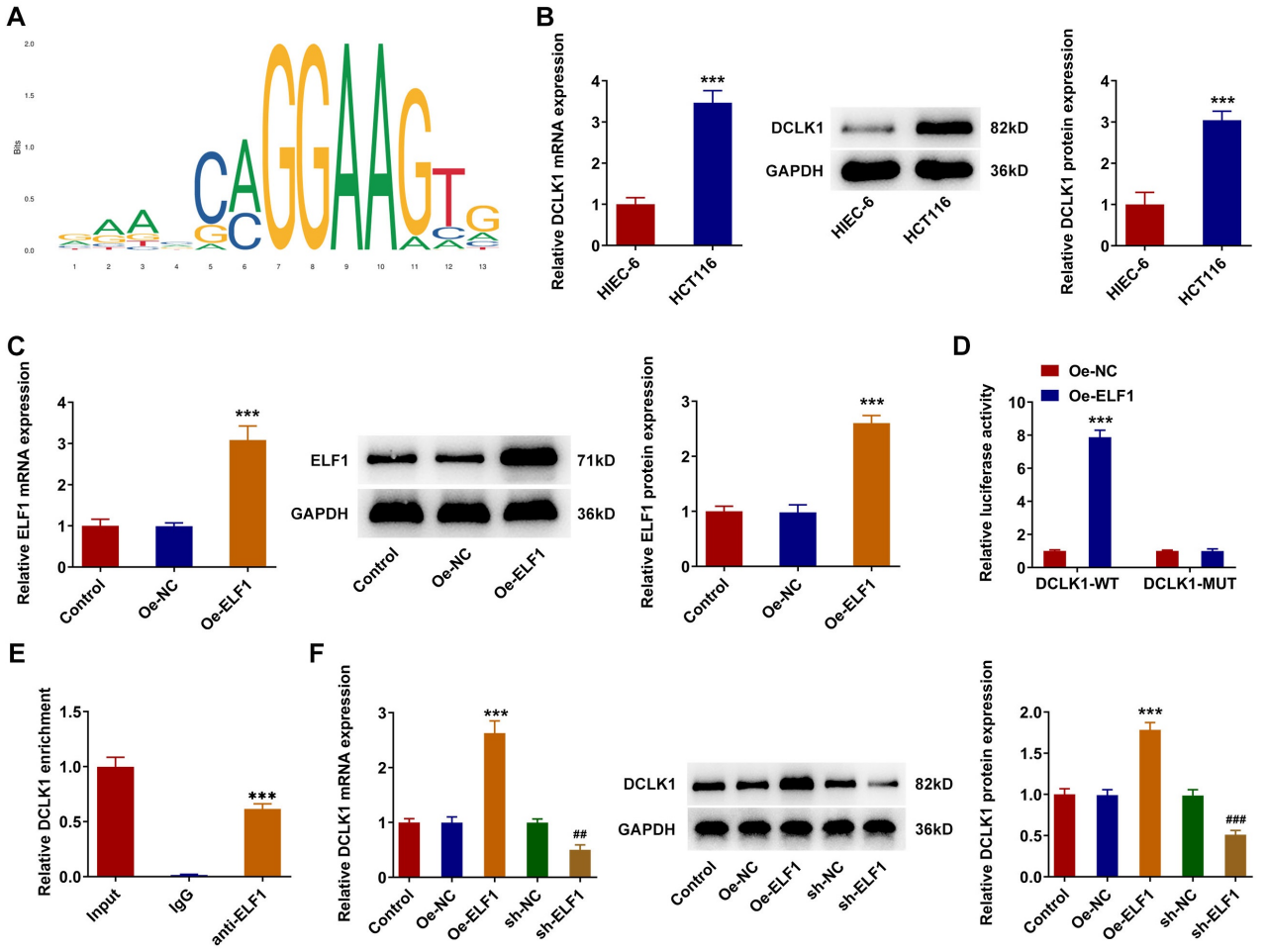

Fig. 4. ELF1 promotes the transcription of DCLK1 (n = 3). (A) The transcription factor ELF1 and DCLK1 promoter binding sites were predicted by the JASPAR database. (B) The expression of DCLK1 in CRC cells was detected by RT-qPCR and western blotting. (C) ELF1 overexpression plasmid was constructed, and transfection efficacy was detected by RT-qPCR and western blotting. (D) Luciferase report assay detected the activity of the DCLK1 promoter after overexpressing ELF1. (E) The binding of ELF1 with DCLK1 promoter was detected by ChIP. (F) The expression of DCLK1 in CRC cells was detected by RT-qPCR and western blotting after transfection. ***$p < 0.001$ vs HIEC-6, Oe-NC or IgG; $^{\#\#}p < 0.01$, $^{\#\#\#}p < 0.001$ vs sh-NC. DCLK1, Doublecortin Like Kinase 1; IgG, immunoglobulin G; ChIP, Chromatin Immunoprecipitation.

with the findings proposed by Chen *et al.* [16], which showed that *ELF1* mediates CCL2/CCR2 signaling to accelerate nasopharyngeal carcinoma cell proliferation and metastasis, and in line with the research of Huang *et al.* [17], presenting that *ELF1* is engaged in tumor-triggered new angiogenesis in melanoma.

To investigate the regulatory mechanism of *ELF1* on CRC, the binding sites of the DCLK1 promoter with ELF1 transcription factor were predicated by the JASPAR database. In this paper, the binding ability between the DCLK1 promoter and ELF1 was confirmed by relevant mechanism assays. *DCLK1*, a kinase concerned with microtubules, is increased in various tumors. Previous studies have shown that *DCLK1* upregulation can promote aggressive cell growth, epithelial-mesenchymal transition (EMT), and metastasis in cancers, such as liner, CRC, and pancreatic [18–20]. In our experiment, DCLK1 expression was increased in HCT116 cells, consistent with results from a previous study [21]. With this regard, it is reasonable to speculate that there is a regulatory effect between *ELF1* and *DCLK1* in CRC. We found that after the transfection of Oe-ELF1 in HCT116 cells, DCLK1 expression was increased, while *ELF1* knockdown decreased DCLK1 expression. These findings underline that *ELF1* positively regulated DCLK1 expression in CRC cells.

Therefore, we interfered with *ELF1* in cells and concurrently increased DCLK1 in HCT116 cells. It was found that *DCLK1* upregulation could counteract the inhibitory effects of *ELF1* interference on the malignant progression and stemness of CRC cells. A previous study has shown that *DCLK1* promotes stemness and aggression in CRC through XRCC5/COX2 axis [21]. *DCLK1* regulates cell stemness to

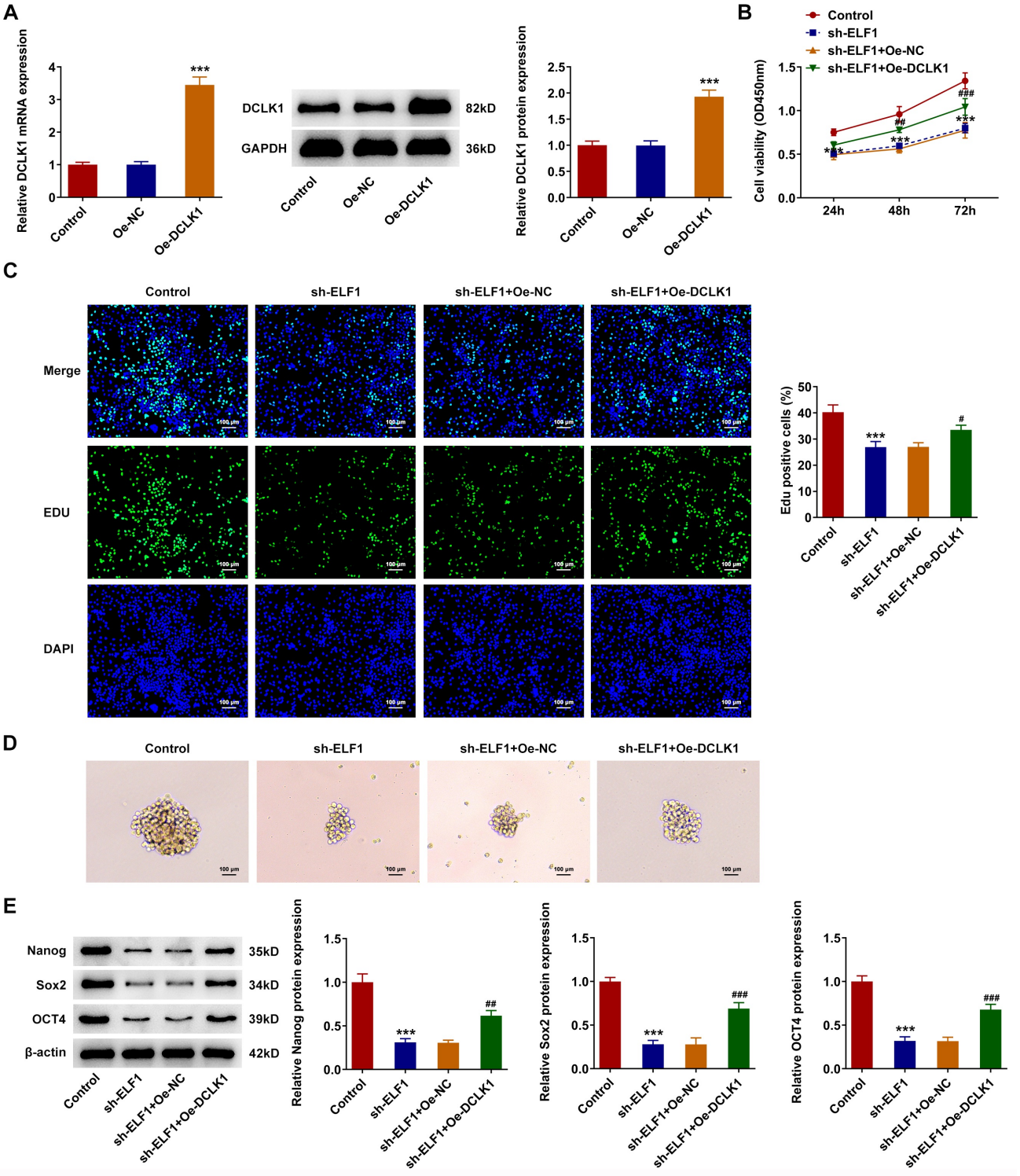

Fig. 5. ELF1 up-regulates DCLK1 expression to promote the proliferation and stemness of CRC (n = 3). (A) DCLK1 overexpression plasmid was constructed, and the transfection efficiency was examined by RT-qPCR and western blotting. ***$p < 0.001$ vs Oe-NC. (B) Cell viability was measured by CCK-8 assay. (C) EdU staining detected cell proliferation (100 μm). (D) Sphere formation assay detected the sphere-forming ability of cells (100 μm). (E) Western blotting analysis detected the expression of cell stem-related proteins Nanog, Sox2, and OCT4. ***$p < 0.001$ vs Control; $^{\#}p < 0.05$, $^{\#\#}p < 0.01$, $^{\#\#\#}p < 0.001$ vs sh-ELF1 + Oe-NC. DCLK1, Doublecortin Like Kinase 1; EdU, 5-Ethynyl-2′-deoxyuridine.

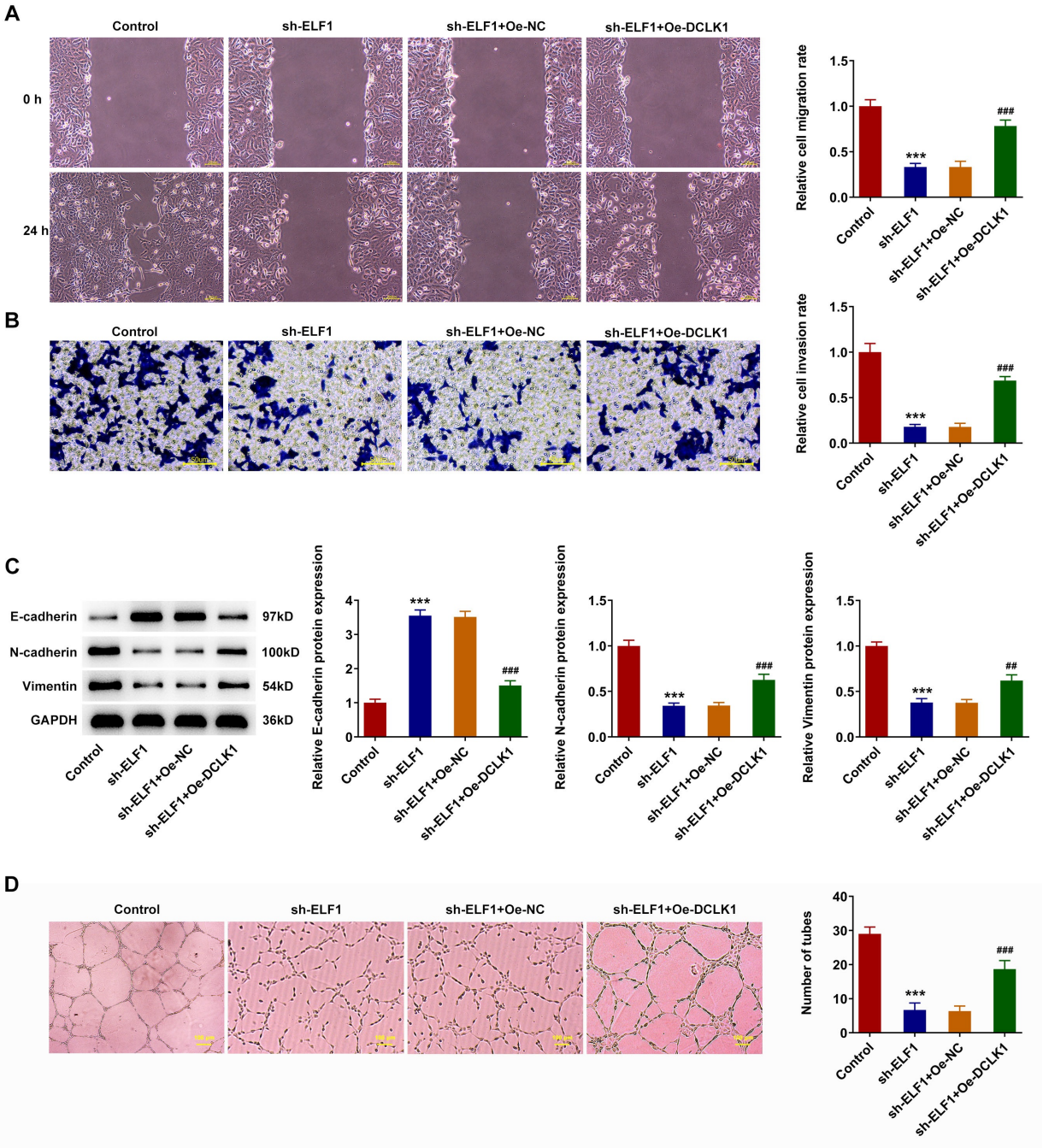

Fig. 6. ELF1 up-regulates DCLK1 expression to promote the invasion, migration, and angiogenesis of CRC (n = 3). The migration and invasion of CRC cells were measured by wound healing (A, 100 μm) and transwell assay (B, 50 μm). (C) Western blotting detected the expressions of ETM-related proteins. (D) Tubule formation assay detected tubule forming ability of HUVECs (100 μm). ***$p <$ 0.001 vs Control; $^{\#\#}p < 0.01$, $^{\#\#\#}p < 0.001$ vs sh-ELF1 + Oe-NC.

reduce 5-fluorouracil sensitivity in CRC via the CCAR1/β-catenin pathway [22]. *DCLK1* binds with microRNA to mediate pluripotent and angiogenic factors in pancreatic cancer [23]. In addition, *ELF1* transcriptionally activates EMI1 and promotes glioma cell angiogenesis [24]. The above results are consistent with the experimental results of our paper.

However, the limitations of the current research should not be overlooked. Firstly, the roles of *ELF1* and *DCLK1* in CRC have only been confirmed in HCT116 cells so far. In the future, more types of CRC cell lines should be included to validate the role of *ELF1* in CRC fully. More importantly, compared to *in vivo* experiments, *in vitro* experiments have significant limitations. Therefore, it is essential to establish a CRC nude mouse model for further

verification of the role of *ELF1* in CRC *in vivo*. In addition, it is worth further exploring the different signaling mechanisms involved in the roles of *ELF1* and *DCLK1* in CRC.

Conclusion

In summary, the present study explored the role of *ELF1* in CRC through *in vitro* experiments and confirmed the interaction between *ELF1* and *DCLK1* in CRC cells. It can be concluded that *ELF1* up-regulates DCLK1 expression to promote the malignant progression and stemness of CRC. This provides a preliminary theoretical basis for the development of new targets for the treatment of CRC.

Availability of Data and Materials

The datasets utilized and/or analyzed in the present work can be obtained from the corresponding author on reasonable request.

Author Contributions

FZ designed the thought of the experiment. DZ, XT, HY, SX and YL operated the experiment. FZ, DZ, XT and HY processed the experimental data and ensured the authenticity and accuracy of the experimental data. DZ drafted the manuscript and all authors were involved in the drafting and critical revision of the manuscript. All authors have read and approved the final manuscript. All authors have participated sufficiently in the work and agreed to be accountable for all aspects of the work.

Ethics Approval and Consent to Participate

Not applicable.

Acknowledgment

Not applicable.

Funding

Hunan Provincial Health Commission scientific research project (202103031598). Youth Fund of Hunan Provincial Department of Education (No.21B0093).

Conflict of Interest

The authors declare no conflict of interest.

References

[1] Shen C, Tannenbaum D, Horn R, Rogers J, Eng C, Zhou S, *et al*. Overall Survival in Phase 3 Clinical Trials and the Surveillance, Epidemiology, and End Results Database in Patients With Metastatic Colorectal Cancer, 1986–2016: A Systematic Review. JAMA Network Open. 2022; 5: e2213588.

[2] Zhang XH, Zhou JQ, Wei Q, Li J, Xu T, Bai CM, *et al*. Genomic Alterations and Clinical Characterization in Chinese Patients with Metastatic Colorectal Cancer. Discovery Medicine. 2024; 36: 1477–1485.

[3] Perri F, Longo F, Giuliano M, Sabbatino F, Favia G, Ionna F, *et al*. Epigenetic control of gene expression: Potential implications for cancer treatment. Critical Reviews in Oncology/Hematology. 2017; 111: 166–172.

[4] Zhang J, Shen Z, Song Z, Luan J, Li Y, Zhao T. Drug Response Associated With and Prognostic lncRNAs Mediated by DNA Methylation and Transcription Factors in Colon Cancer. Frontiers in Genetics. 2020; 11: 554833.

[5] Clark CR, Maile M, Blaney P, Hellweg SR, Strauss A, Durose W, *et al*. Transposon mutagenesis screen in mice identifies TM9SF2 as a novel colorectal cancer oncogene. Scientific Reports. 2018; 8: 15327.

[6] Paczkowska J, Soloch N, Bodnar M, Kiwerska K, Janiszewska J, Vogt J, *et al*. Expression of ELF1, a lymphoid ETS domain-containing transcription factor, is recurrently lost in classical Hodgkin lymphoma. British Journal of Haematology. 2019; 185: 79–88.

[7] Hu M, Li H, Xie H, Fan M, Wang J, Zhang N, *et al*. ELF1 Transcription Factor Enhances the Progression of Glioma via ATF5 promoter. ACS Chemical Neuroscience. 2021; 12: 1252–1261.

[8] Wang L. ELF1-activated FOXD3-AS1 promotes the migration, invasion and EMT of osteosarcoma cells via sponging miR-296-5p to upregulate ZCCHC3. Journal of Bone Oncology. 2020; 26: 100335.

[9] Chandrashekar DS, Karthikeyan SK, Korla PK, Patel H, Shovon AR, Athar M, *et al*. UALCAN: An update to the integrated cancer data analysis platform. Neoplasia (New York, N.Y.). 2022; 25: 18–27.

[10] Castro-Mondragon JA, Riudavets-Puig R, Rauluseviciute I, Lemma RB, Turchi L, Blanc-Mathieu R, *et al*. JASPAR 2022: the 9th release of the open-access database of transcription factor binding profiles. Nucleic Acids Research. 2022; 50: D165–D173.

[11] Chen S, Fan L, Lin Y, Qi Y, Xu C, Ge Q, *et al*. Bifidobacterium adolescentis orchestrates CD143$^+$ cancer-associated fibroblasts to suppress colorectal tumorigenesis by Wnt signaling-regulated GAS1. Cancer Communications (London, England). 2023; 43: 1027–1047.

[12] Skvortsova I. Cancer Stem Cells: What Do We Know about Them? Cells. 2021; 10: 1528.

[13] Kuşoğlu A, Biray Avcı Ç. Cancer stem cells: A brief review of the current status. Gene. 2019; 681: 80–85.

[14] Wang L, Tang D, Wu T, Sun F. ELF1-mediated LUCAT1 promotes choroidal melanoma by modulating RBX1 expression. Cancer Medicine. 2020; 9: 2160–2170.

[15] Qiao C, Qiao T, Yang S, Liu L, Zheng M. SNHG17/miR-384/ELF1 axis promotes cell growth by transcriptional regulation of CTNNB1 to activate Wnt/β-catenin pathway in oral squamous cell carcinoma. Cancer Gene Therapy. 2022; 29: 122–132.

[16] Chen CH, Su LJ, Tsai HT, Hwang CF. ELF-1 expression in nasopharyngeal carcinoma facilitates proliferation and metastasis of cancer cells via modulation of CCL2/CCR2 signaling. Cancer Management and Research. 2019; 11: 5243–5254.

[17] Huang X, Brown C, Ni W, Maynard E, Rigby AC, Oettgen P. Critical role for the Ets transcription factor ELF-1 in the development of tumor angiogenesis. Blood. 2006; 107: 3153–3160.

[18] Fan M, Qian N, Dai G. Expression and prognostic significance of doublecortin-like kinase 1 in patients with hepatocellular carcinoma. Oncology Letters. 2017; 14: 7529–7537.

[19] Gzil A, Szylberg Ł, Jaworski D, Dominiak J, Zarębska I, Grzanka D. The Essential Role of DCLK1 in Pathogenesis, Diagnostic Procedures and Prognostic Stratification of Colorectal Cancer. Anticancer Research. 2019; 39: 2689–2697.

[20] Qu D, Johnson J, Chandrakesan P, Weygant N, May R, Aiello N, *et al*. Doublecortin-like kinase 1 is elevated serologically in pancreatic ductal adenocarcinoma and widely expressed on circulating tumor cells. PLoS ONE. 2015; 10: e0118933.

[21] Kim JH, Park SY, Jeon SE, Choi JH, Lee CJ, Jang TY, *et al*. DCLK1 promotes colorectal cancer stemness and aggressiveness via the XRCC5/COX2 axis. Theranostics. 2022; 12: 5258–5271.

[22] Wang L, Zhao L, Lin Z, Yu D, Jin M, Zhou P, *et al*. Targeting DCLK1 overcomes 5-fluorouracil resistance in colorectal cancer through inhibiting CCAR1/β-catenin pathway-mediated cancer stemness. Clinical and Translational Medicine. 2022; 12: e743.

[23] Sureban SM, May R, Qu D, Weygant N, Chandrakesan P, Ali N, *et al*. DCLK1 regulates pluripotency and angiogenic factors via microRNA-dependent mechanisms in pancreatic cancer. PLoS ONE. 2013; 8: e73940.

[24] Wang M, Yang C, Liu X, Zheng J, Xue Y, Ruan X, *et al*. An upstream open reading frame regulates vasculogenic mimicry of glioma via ZNRD1-AS1/miR-499a-5p/ELF1/EMI1 pathway. Journal of Cellular and Molecular Medicine. 2020; 24: 6120–6136.